Control of Nonholonomic Electrically-Driven Tractor-Trailer Wheeled Robots based on Adaptive Partial Linearization

Bahram Tarvirdeizadeh[1], Khalil Alipour[1*], Sotirios Spanogianopoulos[2]

1. Advanced Service Robots(ASR) Laboratoary, Depatment of Mechatronics Eng., Faculty of New Sciences and Technologies, University of Tehran, Tehran, Iran.

2. Kent University, England.

ARTICLE INFO

Article history:

Keywords:
Wheeled Mobile Robot,
Tractor-Trailer,
Motion Control,
System Identification

ABSTRACT

Wheeled Mobile Robots (WMRs) are simple, easy to move on hard and level terrain and can be controlled effectively. Due to these merits, many researchers have studied the challenges of WMRs. To improve the payload transportation capability of wheeled vehicles, one or several platform, named as trailer, may towed to a tractor wheeled platform. In the current paper, for the first time, the motion control of such tractor trailer systems is addressed while the actuator dynamics is considered. Toward this goal, the system kinematics and dynamics will be derived and will be coupled to its actuators model. To control the considered nonholonomic system, the technique of input-output feedback linearization along with look-ahead point notion will be utilized. Besides, some of the imprecise parameters in the proposed model-based controller are identified in an on-line manner. The obtained computer simulation results support the soundness of the proposed controller.

1. Introduction

Robotic systems provide different services in various environments based on the mission requirements. The robotic systems may consist of dexterous manipulation and locomotion divisions. While the manipulation part provides the capability of the dexterous operation on the environment, the locomotion is responsible for the robot motion in the environment. Based on the environment, and the mission requirements, the robot locomotion may be different. The robots could be flying, move on the surface (ground) or travel underwater. The ground robots locomotion would mainly be wheeled, legged, tracked or some combination of the three aforementioned mechanisms.

Among various locomotion mechanisms of the robots, the wheels are simple, easy to control and fast for motion over hard even terrains. These advantages have encouraged the researchers to focus on solving the challenges of the wheeled robots, [1], [2]. While the single-platform wheeled robots are advantageous, their payload carrying capacity is limited. In order to improve the payload carrying capacity and preserving the system maneuverability, another wheeled platform(s) is (are) connected to the active platform. Such wheeled robots are called tractor-trailer wheeled robots (TTWRs). The active platform which provide the overall system driving is called tractor while the other wheeled platforms which are passive are called trailers, see Fig. 1.

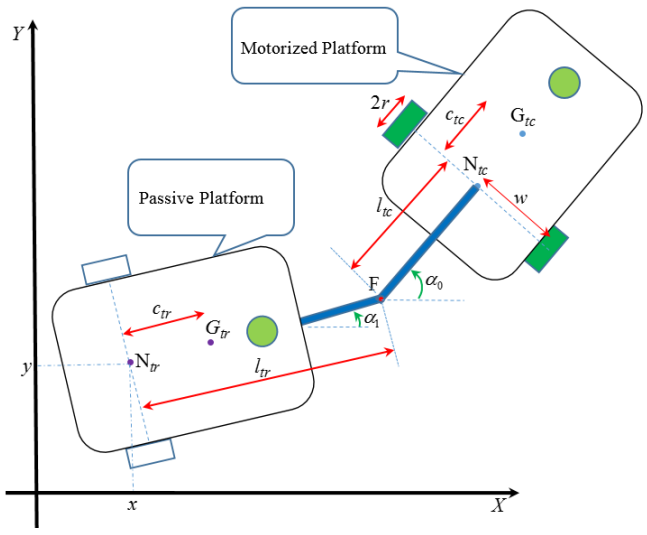

Figure 1. The considred tractor-triler wheeld robot system

While such systems have been studied from the view point of motion planning [3-5], few works have been presented in the field of automatic control.

In the motion control field of the wheeled robots, there exist three types of problem including trajectory tracking, path following and posture stabilization [6]. The aim of trajectory tracking is that the desired trajectories associated with the coordinates of a reference point of the robot could be tracked. In [7], considering the trailer linear velocity and tractor angular velocity as control inputs, the trajectories of a reference point of the trailer have been controlled. To this end, the linear model predictive control technique has been utilized. In [8], first a Lyapunov-based kinematic controller has been designed for TTWRs. Then, a dynamic controller has been designed such that it can provide the required velocities of the kinematic controller using torques of the tractor wheels. In [9], the trajectory tracking of TTWRs has been realized using the notion of Modified Transpose Jacobian (MTJ) controller. One of the advantages of the use of MTJ is its simplicity and its independency from the robot dynamic model parameters. In [10], a TTWR is considered in which the trailer wheels are spherical. The considered under-actuated system is modeled and then is controlled using a physics based PID controller. The stability of the controller has been proven using the Lyapunov second method.

While few controllers have just been recently proposed to control TTWRs motion, most of them assume that the precise parameters of the robot are available. Besides, most of them ignore the actuators dynamics. Consequently, in the percent work, the considered TTWR is modeled and controlled while the actuator dynamics is taken into account. Besides, the values of some of the uncertain parameters of the robot and its actuators are identified. To control the robot, the input-output feedback linearization control technique is utilized adopting the look-ahead control strategy [11].

The rest of the present article is arranged as follows. In Section 2, the considered system is described and its kinematics and dynamics are derived. Then, in Section 3, the nonlinear developed controller as well as identification methods are introduced. In Section 4, the obtained simulation results are discussed. Some conclusions will be given in the last section.

2. system Desciption and its kinematics and dynamics

2.1. System Describtion

The considered system is composed of two wheeled platforms, as shown in Fig. 1. Each platform contains there wheels where two of them are conventional wheels and mounted at the rear of the platform. The third wheel is of type spherical and is utilized to enhance the equilibrium of the system. The wheeled platform whose rear wheels are active is named as the tractor while the other platform is called trailer. Since the two real wheels of the tractor are independently driven by electric DC motors, the tractor is of type differentially-driven platform and kinematically equivalent to unicycle type mobile robot, [12].

In Fig. 1, the various geometrical parameters of the robot is shown. N_{tc} and N_{tr} represent the midpoint of the rear axle of the tractor and the trailer, respectively. Also, x and y denote the Cartesian coordinates of point N_{tr} in inertial XY frame. Besides, α_0 and α_1 denote the heading angle of the tractor and the trailer with respect to X axis of inertial frame, respectively. Moreover, G_{tc} and G_{tr} denote the center of mass of the tractor and the trailer, respectively. In addition, w and r indicate the half of distance between center of wheels and the radius of wheels, respectively.

2.2. System Kinematics and Dynamics

To describe the system configuration, the following entities of vector $\boldsymbol{\mu}$ are selected

$$\boldsymbol{\mu} = [x \quad y \quad \alpha_1 \quad \alpha_0]^{\mathrm{T}} \tag{1}$$

It is recalled that the elements of vector $\boldsymbol{\mu}$ was explained in the former subsection. Herein, it is tried to examine the system kinematics and also derive the relation between the angular velocity of actuation wheels and the generalized velocities, i.e. $\dot{\boldsymbol{\mu}}$. If the angular displacements of the tractor right and left active wheels are denoted by δ_r and δ_l , respectively, then the following relations can be written

$$\begin{aligned} v_{rw} &= \mathrm{r}\,\dot{\delta}_r [\cos\alpha_0 \quad \sin\alpha_0]^{\mathrm{T}} \\ v_{lw} &= \mathrm{r}\,\dot{\delta}_l [\cos\alpha_0 \quad \sin\alpha_0]^{\mathrm{T}} \end{aligned} \tag{2}$$

where v_{rw} and v_{lw} denote the linear velocity of the right and the left active wheels of the tractor, respectively. Notice that the above relations are correct provided that the wheels are subject to pure rolling condition. Also, as the linear velocity of the point N_{tc} relative to the tractor active wheels is perpendicular to the line connecting the aforementioned wheels centers, then it can be concluded that

$$\tan\alpha_0 = \dot{y}_{tc} / \dot{x}_{tc} \tag{3}$$

or

$$\dot{x}_{tc} \sin\alpha_0 - \dot{y}_{tc} \cos\alpha_0 = 0 \tag{4}$$

where x_{tc} and y_{tc} denote the Cartesian coordinates of the point N_{tc} in XY frame. Also, the following relations hold between coordinates of the points N_{tc} and N_{tr} .

$$\begin{aligned} x_{tc} &= x + l_{tr} c\alpha_1 + l_{tc} c\alpha_0 \\ y_{tc} &= x + l_{tr} s\alpha_1 + l_{tc} s\alpha_0 \end{aligned} \tag{5}$$

where c and s stand for functions cos and sin, respectively. By substituting (5) into (4), the following result is obtained.

$$\dot{x} \sin\alpha_0 - \dot{y} \cos\alpha_0 - \dot{\alpha}_1 l c(\alpha_0 - \alpha_1) = 0 \tag{6}$$

The recent relation is a non-integrable constraint and hence the TTWR is a nonholonomic mechanical system.
By similar argument about the linear velocity of point N_{tr} , the following results is achieved.

$$\dot{x}\sin\alpha_1 - \dot{y}\cos\alpha_1 = 0 \tag{7}$$

The above relation is also nonholonomic which along with (6) can be written in the following compact matrix format.

$$\boldsymbol{\zeta}(\boldsymbol{\mu})\dot{\boldsymbol{\mu}} = \mathbf{0} \tag{8}$$

in which

$$\boldsymbol{\zeta} = \begin{bmatrix} \sin\alpha_0 & -\cos\alpha_0 & -l\cos(\alpha_0-\alpha_1) & 0 \\ \sin\alpha_1 & -\cos\alpha_1 & 0 & 0 \end{bmatrix} \tag{9}$$

where $l = l_{tr}$ if it is assumed that the on-axle hitching case is examined, i.e. $l_{tc} = 0$.

By writing the kinematic equation relating the linear velocity of the right and the left active wheels of tractor, then the following result is obtained.

$$\dot{\alpha}_0 = \frac{r}{2w}(\dot{\delta}_r - \dot{\delta}_l) \tag{10}$$

If $\upsilon_{N_{tr}}$ is defined as the value (with sign) of the linear velocity of the point N_{tr}, then by velocity analysis of the points N_{tr} and F, the following result can be obtained.

$$\upsilon_{N_{tr}} = \frac{r}{2}(\dot{\delta}_r + \dot{\delta}_l)\cos(\alpha_0 - \alpha_1) \tag{11}$$

considering (10) and (11), the following imaginary kinematic input is defined as

$$\mathbf{u} = \begin{bmatrix} u_1 \\ u_2 \end{bmatrix} = \begin{bmatrix} \upsilon_{N_{tr}} \\ \dot{\alpha}_0 \end{bmatrix} = \boldsymbol{\Lambda}\begin{bmatrix} \dot{\delta}_r \\ \dot{\delta}_l \end{bmatrix}$$
$$\boldsymbol{\Lambda} = \begin{bmatrix} \frac{r}{2}\cos(\alpha_0-\alpha_1) & \frac{r}{2}\cos(\alpha_0-\alpha_1) \\ \frac{r}{2w} & -\frac{r}{2w} \end{bmatrix} \tag{12}$$

As seen the map between virtual kinematic input $\mathbf{u}$ and active wheels' angular velocities is one-to-one. Hence, they are equivalent and can be utilized interchangeably. Since, the wheels of the trailer do not slip sideways, the following two relations can be written.

$$\begin{aligned} \dot{x} &= u_1\cos\alpha_1 \\ \dot{y} &= u_1\sin\alpha_1 \end{aligned} \tag{13}$$

Considering (10) the magnitude of the velocity of the point N_{tc} (with its sign) can be written in terms of the tractor wheels' velocities as

$$\upsilon_{N_{tc}} = \frac{r}{2}(\dot{\delta}_r + \dot{\delta}_l) \tag{14}$$

By recalling the point that in the present study, $l_{tc} = 0$, and writing the linear velocity relation between points N_{tc} and N_{tr}, and using (14), (13), and (12), the following result is concluded.

$$\dot{\alpha}_1 = \frac{1}{l}\tan(\alpha_0 - \alpha_1)\,\mathrm{u}_1 \tag{15}$$

The relations (13), (15) and (10) using (12) can be written in the following compact from.

$$\dot{\boldsymbol{\mu}} = \mathbf{Q}(\boldsymbol{\mu})\cdot\mathbf{u} \tag{16}$$

where

$$\mathbf{Q}^{\mathrm{T}} = \begin{bmatrix} \mathrm{c}\alpha_1 & s\alpha_1 & \frac{1}{l}\tan(\alpha_0-\alpha_1) & 0 \\ 0 & 0 & 0 & 1 \end{bmatrix} \tag{17}$$

As seen, (16) indicates that the first-order kinematics of the system is driftless, [12]. Also, one can conclude that the two independent columns of matrix $\mathbf{Q}$ span the admissible generalized velocities $\dot{\boldsymbol{\mu}}$.

Now, the system dynamics model is extracted. In this regard, first the system Lagrangian is obtained. As the robot system has planar motion its Lagrangian L can be written as below if the wheels' mass is ignored.

$$L(\boldsymbol{\mu},\dot{\boldsymbol{\mu}}) = \frac{1}{2}m_{tc}\upsilon_{G_{tc}}^2 + \frac{1}{2}I_{tc}\dot{\alpha}_0^2 + \frac{1}{2}m_{tr}\upsilon_{G_{tr}}^2 + \frac{1}{2}I_{tr}\dot{\alpha}_1^2 \tag{18}$$

where m_{tc} and m_{tr} represent the tractor and the trailer masses, respectively. Also, I_{tc} and I_{tr} represent the tractor and the trailer mass moments of inertia about their associated center of mass, respectively. Besides, $\upsilon_{G_{tc}}$ and $\upsilon_{G_{tr}}$ denote the linear velocity value of center of masses of the tractor and the trailer, respectively. Note that if the right-hand side of the above equation is written in terms of $\boldsymbol{\mu}$ and $\dot{\boldsymbol{\mu}}$, then by its substitution in the constrained Lagrange formulation, the following is resulted.

$$\mathbf{A}(\boldsymbol{\mu})\ddot{\boldsymbol{\mu}} + \mathbf{n}(\boldsymbol{\mu},\dot{\boldsymbol{\mu}})\,\dot{\boldsymbol{\mu}} = \mathbf{E}(\boldsymbol{\mu})\mathbf{T} + \boldsymbol{\zeta}^{\mathrm{T}}(\boldsymbol{\mu})\boldsymbol{\lambda} \tag{19}$$

where $\mathbf{A}$ represents the configuration dependent mass/inertia matrix and $\mathbf{n}\dot{\boldsymbol{\mu}}$ is the vector containing the Coriolis and centripetal forces, [13]. Besides, $\mathbf{E}$ is input matrix which transfers the effect of the wheels actuating torques $\mathbf{T}$ to the generalized forces. Also, $\boldsymbol{\lambda}$ denotes the 2×1 vector of Lagrange multipliers. Now, by premultiplication of the above relation by $\mathbf{Q}^{\mathrm{T}}$, and substituting of $\dot{\boldsymbol{\mu}}$ by the right-hand side of (15), the following reduced dynamics model is achieved.

$$\bar{\mathbf{M}}\dot{\mathbf{u}} + \bar{\mathbf{C}}(\boldsymbol{\mu},\mathbf{u})\mathbf{u} = \mathbf{Q}^{\mathrm{T}}\mathbf{E}(\boldsymbol{\mu})\mathbf{T} \tag{20}$$

where

$$\begin{aligned} \bar{\mathbf{M}}(\boldsymbol{\mu}) &= \mathbf{Q}^{\mathrm{T}}\mathbf{A}(\boldsymbol{\mu})\mathbf{Q} \\ \bar{\mathbf{C}}(\boldsymbol{\mu},\mathbf{u}) &= \mathbf{Q}^{\mathrm{T}}\mathbf{A}(\boldsymbol{\mu})\dot{\mathbf{Q}} + \mathbf{Q}^{\mathrm{T}}\,\mathbf{n}(\boldsymbol{\mu},\dot{\boldsymbol{\mu}})\mathbf{Q} \end{aligned} \tag{21}$$

Note that (20) is obtained since the columns of the matrix $\mathbf{Q}$ belong to the null-space of the matrix $\boldsymbol{\zeta}(\boldsymbol{\mu})$ and consequently, $\boldsymbol{\zeta}\mathbf{Q} = \mathbf{0}$.

2.3. Actuator Model

The relation between the voltage source of armature circuit and its current can be described by the following first-order differential equation, [13].

$$l_A \dot{i}_A + R_A i_A = v_A - k_e \dot{\alpha}_m \tag{22}$$

where l_A and R_A denote, the inductance and resistance of the armature circuit, respectively. Besides, i_A and v_A denote the current and source voltage of the armature windings, respectively. Also, k_e indicate the back-electromotive force constant of the motor and $\dot{\alpha}_m$ shows the angular velocity of the motor. In motors, the inductances are ignorable and the produced torque (τ_m) is related to the current flows in the armature windings as $\tau_m = k_m i_A$. Note that k_m is the motor torque constant. Hence, (20) is written as

$$\frac{R_A}{k_m}\tau_m = v_A - k_e \dot{\alpha}_m \tag{23}$$

If the motor is not direct drive and connected to the load via a gear reduction module then the following result is obtained

$$\frac{R_A}{K_m}\kappa\tau = v_A - \frac{k_e}{\kappa}\dot{\delta} \tag{24}$$

where $\kappa > 1$ is the ratio of the gear reduction module. Moreover, τ and $\dot{\delta}$ denote the torque and angular velocity delivered to the load.

If it is assumed that the tractor motors and their associated gearboxes are similar, then by applying (24) to the right and the left motors of the tractor, the following result is achieved.

$$\mathbf{T} = \begin{bmatrix} \tau_r \\ \tau_l \end{bmatrix} = \gamma_1 \begin{bmatrix} v_{A_r} \\ v_{A_l} \end{bmatrix} - \gamma_2 \begin{bmatrix} \dot{\delta}_r \\ \dot{\delta}_l \end{bmatrix} \tag{25}$$

where

$$\gamma_1 = \frac{k_m}{\kappa R_A}, \quad \gamma_2 = \frac{k_e k_m}{\kappa^2 R_A} \tag{26}$$

Substituting (12) into (25), the following result is obtained.

$$\mathbf{T} = \begin{bmatrix} \tau_r \\ \tau_l \end{bmatrix} = \gamma_1 \begin{bmatrix} v_{A_r} \\ v_{A_l} \end{bmatrix} - \gamma_2 \mathbf{\Lambda}^{-1}\mathbf{u} \tag{27}$$

If the right hand side of the above relation is substituted for $\mathbf{T}$ in (20), then the following relation is achieved.

$$\tilde{\mathbf{M}}(\boldsymbol{\mu})\cdot\dot{\mathbf{u}}(t) + \tilde{\mathbf{C}}(\boldsymbol{\mu},\dot{\boldsymbol{\mu}})\cdot\mathbf{u}(t) = \gamma_1\tilde{\mathbf{B}}(\boldsymbol{\mu})\cdot\mathbf{v}_a \tag{28}$$

where

$$\begin{aligned} &\tilde{\mathbf{M}} = \bar{\mathbf{M}} \\ &\mathbf{v}_a = \begin{bmatrix} v_{A_r} \\ v_{A_l} \end{bmatrix} \\ &\tilde{\mathbf{B}}(\boldsymbol{\mu}) = \mathbf{Q}^{\mathrm{T}}\mathbf{E}(\boldsymbol{\mu}) \\ &\tilde{\mathbf{C}} = \bar{\mathbf{C}}(\boldsymbol{\mu},\mathbf{u}) + \gamma_2\mathbf{Q}^{\mathrm{T}}\mathbf{E}(\boldsymbol{\mu})\mathbf{\Lambda}^{-1} \end{aligned} \tag{29}$$

3. feedback linearization control and system Identification

In order to design a trajectory tracking controller for the system, the dynamical equation of the system should be considered. The $\tilde{\mathbf{M}}$, $\tilde{\mathbf{C}}$ and $\tilde{\mathbf{B}}$ matrices, can be expressed as follows.

$$\begin{aligned} \tilde{\mathbf{M}}(\boldsymbol{\mu}) &= \begin{bmatrix} M_s + \frac{I_{tr}}{l^2}\tan^2(\alpha_0 - \alpha_1) & 0 \\ 0 & I_{tc} \end{bmatrix} \\ \tilde{\mathbf{C}}(\boldsymbol{\mu},\dot{\boldsymbol{\mu}}) &= \begin{bmatrix} c_{11} & -c_{12} \\ c_{12} & 2\gamma_2\frac{w^2}{r^2} \end{bmatrix} \\ \tilde{\mathbf{B}}(\boldsymbol{\mu}) &= \frac{1}{r}\begin{bmatrix} \frac{1}{\cos(\alpha_0-\alpha_1)} & \frac{1}{\cos(\alpha_0-\alpha_1)} \\ w & -w \end{bmatrix} \end{aligned} \tag{30}$$

where

$$\begin{aligned} M_s &= m_{tc} + m_{tr} \\ c_{12} &= c_{tc} m_{tc} \frac{\dot{\alpha}_0}{\cos(\alpha_0 - \alpha_1)} \\ c_{11} &= -\frac{I_{tr}}{l^2}\dot{\alpha}_1 \frac{\sin(\alpha_0-\alpha_1)}{\cos^3(\alpha_0-\alpha_1)} + \\ &\frac{I_{tr}}{l^2}\dot{\alpha}_0 \frac{\sin(\alpha_0-\alpha_1)}{\cos^3(\alpha_0-\alpha_1)} + 2\frac{\gamma_2}{r^2}\frac{1}{\cos^2(\alpha_0-\alpha_1)} \end{aligned} \tag{31}$$

Considering the kinematics and dynamics of the system, i.e. (28) and (16), the following state space representation will be obtained in control affine arrangement.

$$\dot{\boldsymbol{\eta}} = \begin{bmatrix} \mathbf{Q}\mathbf{u} \\ -\tilde{\mathbf{M}}^{-1}\tilde{\mathbf{C}}\mathbf{u} \end{bmatrix} + \begin{bmatrix} 0 \\ \gamma_1\tilde{\mathbf{M}}^{-1}\cdot\tilde{\mathbf{B}} \end{bmatrix}\mathbf{v}_a \tag{32}$$

where $\boldsymbol{\eta}^T = \begin{bmatrix} \boldsymbol{\mu}^T & \mathbf{u}^T \end{bmatrix}$ is the state vector. This representation helps us to solve the trajectory tracking control problem via feedback linearization approach.

The above equation can be rewritten as follows.

$$\dot{\boldsymbol{\eta}} = h(\boldsymbol{\eta}) + b(\boldsymbol{\eta},\boldsymbol{\theta}) + f(\boldsymbol{\eta},\boldsymbol{\theta})\mathbf{v}_a \tag{33}$$

where we have

$$h(\boldsymbol{\eta})=\begin{bmatrix}\mathbf{Qu}\\0\end{bmatrix},\ b(\boldsymbol{\eta},\boldsymbol{\theta})=\begin{bmatrix}0\\J(\boldsymbol{\eta},\boldsymbol{\theta})\end{bmatrix},$$
$$f(\boldsymbol{\eta},\boldsymbol{\theta})=\gamma_1\begin{bmatrix}0\\F(\boldsymbol{\eta},\boldsymbol{\theta})\end{bmatrix} \tag{34}$$

The goal of control system is that using voltages applied to the wheels motors, i.e. $\mathbf{v}_a$, as control inputs, the trajectory tracked by point N_{tr}, i.e. $[x(t)\ y(t)]$,be as close as possible to the desired reference trajectory. Consequently, $\mathbf{v}_a$ should be adjusted so as

$$\lim_{t\to\infty}\left(x_{des}(t)-x(t)\right)=0\,,\ \lim_{t\to\infty}\left(y_{des}(t)-y(t)\right)=0 \tag{35}$$

The following output are selected as a desired trajectory to be tracked by the system based on look-ahead control approach, [11].

$$C=\begin{bmatrix}x+D\cos(2\alpha_0-\alpha_1)\\y+D\sin(2\alpha_0-\alpha_1)\end{bmatrix} \tag{36}$$

It is recalled that if D in (36), which is named as look-ahead distance, is considered to be zero, then the system will not be input-output linearizable, based on the next equations.

It should be noted that, it is assumed the system is controllable, the internal dynamics of the system is stable, and choosing an appropriate set of output equations, cause the system to be input–output linearizable.

The known approach to find an input–output equation is to frequently differentiate the outputs so that they are explicitly related to inputs. After differentiating (36), the following equations will be obtained.

$$\ddot{\mathbf{C}}=L_h^2\mathbf{C}(\boldsymbol{\eta})+L_bL_h\mathbf{C}(\boldsymbol{\eta})+L_fL_h\mathbf{C}(\boldsymbol{\eta})\cdot\mathbf{v}_a \tag{37}$$

where Lie algebra is utilized in the above equation. Now, the input $\mathbf{v}_a$ can be chosen as

$$\mathbf{v}_a=\left(L_fL_h\mathbf{C}(\boldsymbol{\eta})\right)^{-1}\left[\boldsymbol{\xi}-L_h^2\mathbf{C}(\boldsymbol{\eta})-L_bL_h\mathbf{C}(\boldsymbol{\eta})\right] \tag{38}$$

The above non-linear feedback, linearizes and decouples the system in the following form.

$$\ddot{\mathbf{C}}=\boldsymbol{\xi} \tag{39}$$

where $\boldsymbol{\xi}$ represents the virtual input vector. It can be chosen as

$$\boldsymbol{\xi}=\ddot{\mathbf{C}}_{des}+\mathbf{K}_1\dot{\mathbf{e}}+\mathbf{K}_2\mathbf{e} \tag{40}$$

where $\mathbf{K}_1$ and $\mathbf{K}_2$ are appropriate control gain matrices.

It is worth mentioning that the developed controller (38) is model-based and depends on the robot parameters. In the real world applications, the exact values of the parameters m_{tr}, m_{tr}, r, w and l, are available while the values of parameters related to position of the center of mass, moment of inertia and actuators' constants, such as c_{tc}, I_{tc}, I_{tr}, γ_1 and γ_2, contain uncertainties. Therefore, the exact values of the mentioned parameters will be identified in this study. To this end, the following parameters are considered as unknown values.

$$\boldsymbol{\theta}=\begin{bmatrix}\gamma_1 & I_{tr}/l^2 & I_{tc} & \gamma_2 & c_{tc}m_{tc}\end{bmatrix}^T \tag{41}$$

Applying this notation, Eq. (30) can be rewritten as follows.

$$\tilde{\mathbf{M}}(\boldsymbol{\mu})=\begin{bmatrix}M_s+\theta_2\tan^2(\alpha_0-\alpha_1) & 0\\0 & \theta_3\end{bmatrix}$$
$$\tilde{\mathbf{C}}(\boldsymbol{\mu},\dot{\boldsymbol{\mu}})=\begin{bmatrix}c_{11} & -c_{12}\\c_{12} & 2\theta_4\dfrac{w^2}{r^2}\end{bmatrix} \tag{42}$$
$$\tilde{\mathbf{B}}(\boldsymbol{\mu})=\frac{1}{r}\begin{bmatrix}\dfrac{1}{\cos(\alpha_0-\alpha_1)} & \dfrac{1}{\cos(\alpha_0-\alpha_1)}\\w & -w\end{bmatrix}$$

where $c_{12}=\theta_5\dfrac{\dot{\alpha}_0}{\cos(\alpha_0-\alpha_1)}$ and

$$c_{11}=-\theta_2\dot{\alpha}_1\frac{\sin(\alpha_0-\alpha_1)}{\cos^3(\alpha_0-\alpha_1)}+\theta_2\dot{\alpha}_0\frac{\sin(\alpha_0-\alpha_1)}{\cos^3(\alpha_0-\alpha_1)}$$
$$+2\frac{\theta_4}{r^2}\frac{1}{\cos^2(\alpha_0-\alpha_1)}.$$

Now, the appropriate z_i variables are defined as,

$$z_1=\tan^2(\alpha_0-\alpha_1)\quad,\quad z_2=\dot{\alpha}_1\frac{\sin(\alpha_0-\alpha_1)}{\cos^3(\alpha_0-\alpha_1)}\quad,$$
$$z_3=\dot{\alpha}_0\frac{\sin(\alpha_0-\alpha_1)}{\cos^3(\alpha_0-\alpha_1)}\quad,\quad z_4=\frac{2}{r^2}\frac{1}{\cos^2(\alpha_0-\alpha_1)}\quad,$$
$$z_5=\frac{\dot{\alpha}_0}{\cos(\alpha_0-\alpha_1)}\ \text{and}\ z_6=\frac{1}{\cos(\alpha_0-\alpha_1)}.$$

Substituting above equations into (28) and applying additional mathematical manipulation and some simplifications will resulted to the following equations.

$$\begin{cases}\theta_2Z_2+\theta_4Z_4-\theta_5Z_5-\theta_1Z_1=-M_s\dot{u}_1=y_s\\ \theta_3Z_3+\theta_5Z_7+\theta_4Z_6-\theta_1Z_8=0\end{cases} \tag{43}$$

where Z_i are appropriate regressors, and θ_i are unknown parameters that should be identified *online* during system control. In order to identify these parameters, the Recursive least squares (RLS) estimation method are implemented [14]. In this method, the following equations is utilized to estimate the unknown parameters vector $\boldsymbol{\theta}$.

$$\begin{cases} \hat{\boldsymbol{\theta}}(m+1)=\hat{\boldsymbol{\theta}}(m)+ \\ \quad \dfrac{\mathbf{P}(m)\cdot\mathbf{Z}(m+1)}{1+\mathbf{Z}^T(m+1)\cdot\mathbf{P}(m)\cdot\mathbf{Z}(m+1)}\varepsilon(m+1) \\ \mathbf{P}(m+1)=\mathbf{P}(m)- \\ \quad \dfrac{\left[\mathbf{P}(m)\cdot\mathbf{Z}(m+1)\right]\left[\mathbf{Z}^T(m+1)\cdot\mathbf{P}(m)\right]}{1+\mathbf{Z}^T(m+1)\cdot\mathbf{P}(m)\cdot\mathbf{Z}(m+1)} \end{cases} \quad (44)$$

wehre $\varepsilon(m+1)=y_s(m+1)-\mathbf{Z}^T(m+1)\cdot\boldsymbol{\theta}(m)$, m is the preceding time index, $\mathbf{P}$ is the covariance matrix, $\mathbf{Z}$ is the regressors vector and $\hat{\boldsymbol{\theta}}$ is the estimated unknown parameters vector. It should be noted that, all states of the system are available in real time from measurement.

It should be noted that because of identification process of some of the system parameters, the Eq. (38) should be utilized as follows in the control loop.

$$\mathbf{v}_a=\left(L_{\hat{f}}L_h\mathbf{C}(\boldsymbol{\eta})\right)^{-1}\left[\xi-L_h^2\mathbf{C}(\boldsymbol{\eta})-L_{\hat{b}}L_h\mathbf{C}(\boldsymbol{\eta})\right] \quad (45)$$

The above control input is the final control command to force the system to track the desired trajectory. Figure 2 shows the feedback linearizing control system for the trajectory tracking considering identification of the unknown parameters in the system.

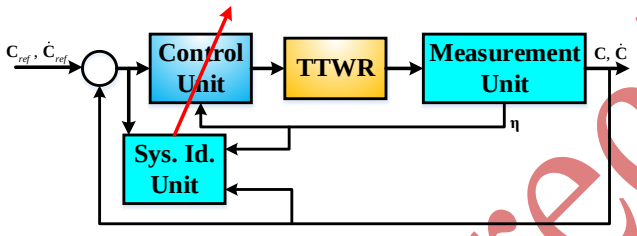

Figure 2. The control schematic of the TTWR system

4. Simulation results

In this part, the simulation results of the implemented controller will be analyzed. The physical parameters of the system are reported in Table 1.

Table 1. The physical parameters of the system

*Param**	*Value*	*Unit*	*Param**	*Value*	*Unit*
m_{tc},m_{tr}	0.9,0.33	kg	c_{tc},c_{tr}	0.29,0	m
I_{tc},I_{tr}	0.0035, 0.00078	kg.m^2	γ_1, γ_2	0.2615, 0.2668	N.m/V, N.msΩ^2/rad
l	0.17	m	w	0.0595	m
r	0.026	m	$\mathbf{K}_1$,$\mathbf{K}_2$	diag(1,1), diag(2,2)	--

*: "*Param*" stands for "*Parameter*"

The desired reference trajectory is considered as a circular path as follows.

$$\begin{bmatrix} x_{des} \\ y_{des} \end{bmatrix}=\begin{bmatrix} 1.7\cos(0.001t^2+0.1) \\ 1.7\sin(0.001t^2+0.1) \end{bmatrix} \quad (46)$$

Notice that based on the above selection for the trajectories of point N_{tr}, the desired outputs are required to be calculated according to (36). In the next simulations the look-ahead distance D=0.17.

The initial condition of the robot is considered as $\boldsymbol{\mu}$ =[-1.8597 m,0.1941 m,-0.1 rad, 0.5 rad] as an arbitrary point in XY plane. Figure 3 shows the trajectory tracking performance of the trailer robot. Figure 4 and Figure 5 show the x and y components of the reference trajectory tracking errors, respectively. It is obvious that the desired trajectory was tracked accurately by the developed controller. Figure 6 and Figure 7 demonstrate the first and the second actuators' output, respectively. Considering Eq. (41), Figure 8 to Figure 12 show the parameters identification process by the adaptation algorithm. It is emphasized that in the simulations, the exact value of these parameters are assumed as $\boldsymbol{\theta}=[0.2615, 0.90, 0.0792, .2668, 0.2610]^T$. The initial guess of the $\boldsymbol{\theta}$ in adaptation algorithm is considered as $\hat{\boldsymbol{\theta}}(0)=[8,10,0.5,0.4,0.4]^T$.

As can be observed in Figure 8 to Figure 12, the considered identification law has estimated all parameters rapidly in less than 1 sec. The final values of the estimated parameters by the developed identification method are as $\hat{\boldsymbol{\theta}}_{identified}=[0.2626,\ 0.9062,\ 0.0802,\ 0.2679,\ 0.2621]^T$.

Comparison.of $\hat{\boldsymbol{\theta}}_{identified}$ with the exact values of theses parameters, $\boldsymbol{\theta}=[0.2615,\ 0.90,\ 0.0792,\ 0.2668,\ 0.2610]^T$, starting from $\hat{\boldsymbol{\theta}}(0)=[8,10,0.5,0.4,0.4]^T$ prove the appropriate performance of the employed identification approach.

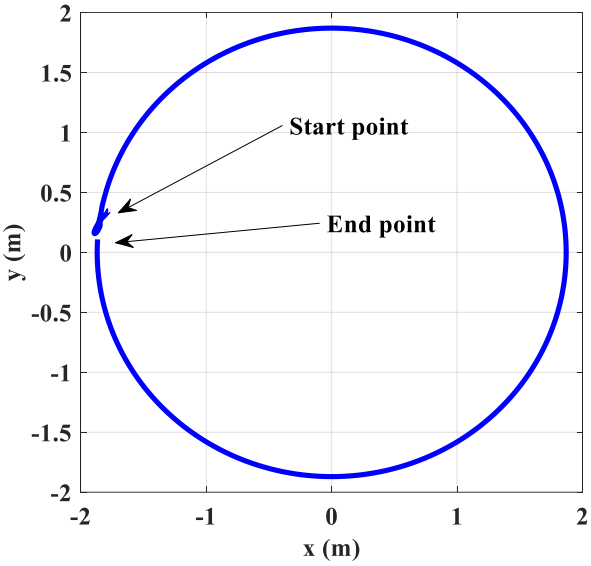

Figure 3. The path tracked by the robot trailer

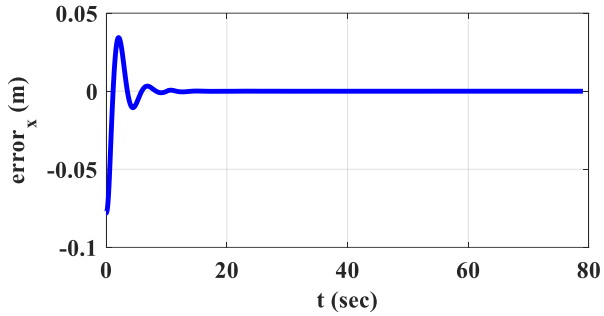

Figure 4. The x component of the reference trajectory tracking error

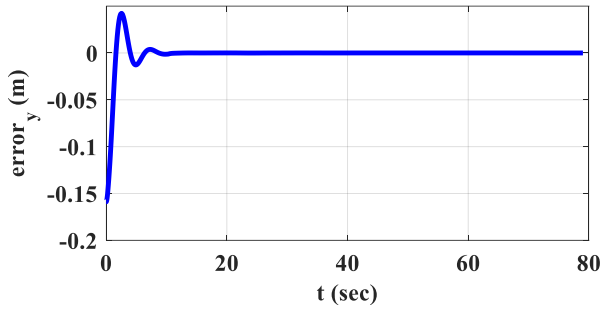

Figure 5. The y component of the reference trajectory tracking error

In order to simulate the real world condition for the TTWR system, the disturbance attenuation performance of the system is analyzed in the simulation tests. To this end, 50% of the control input was added to the system original input to test the disturbance attenuation performance of the developed controller. Figure 13 and Figure 14 show x and y components of the reference trajectory tracking errors considering disturbed input, respectively. Two sets of other simulations considering step-shape and sin-shape disturbances were conducted in the implemented tests. Figure 15 and Figure 16 show x and y components of the reference trajectory tracking errors considering step-shape disturbed input, respectively. The amplitude of this disturbance was 1 mV. Figure 17 and Figure 18 show x and y components of the reference trajectory tracking errors considering sine-shape disturbed input, respectively. The amplitude of this disturbance was 0.5 mV. Moreover, 10% of uncertainty in the masses of the first and the second platforms was added to the system. Figure 19 and Figure 20 show x and y components of the reference trajectory tracking errors considering this type of uncertainty.

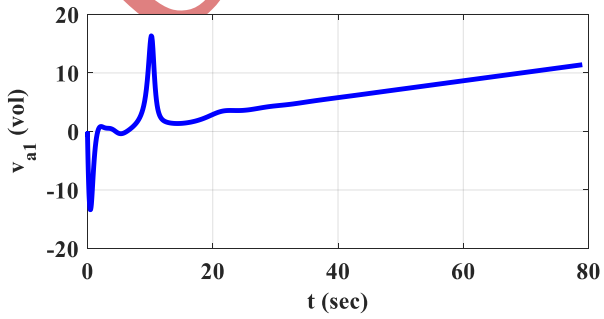

Figure 6. The time history of the first actuator output

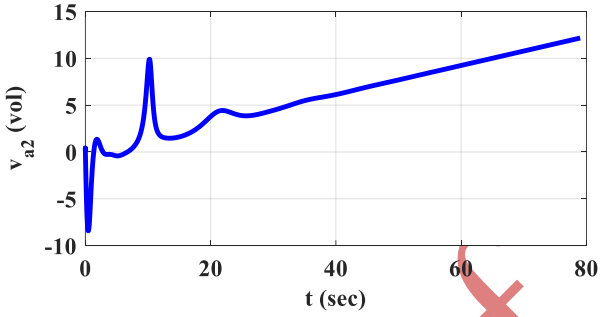

Figure 7. The time history of the second actuator output

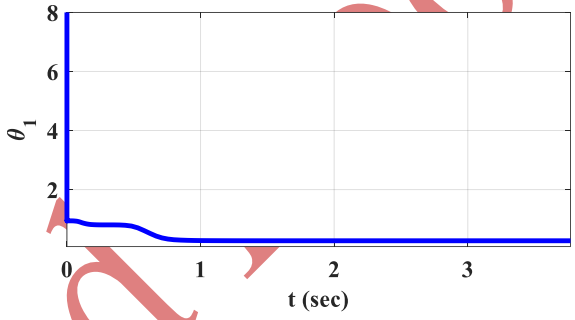

Figure 8. The θ_1 convergence time history

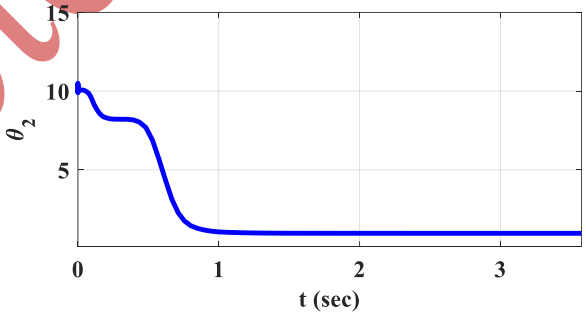

Figure 9. The θ_2 convergence time history

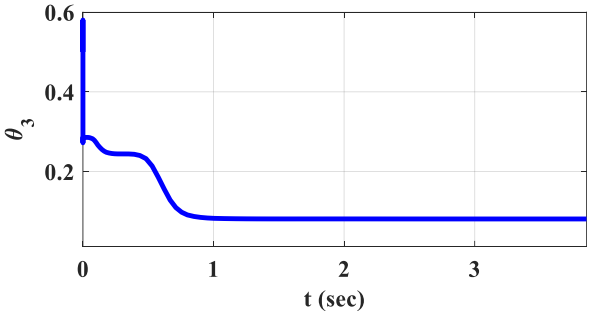

Figure 10. The θ_3 convergence time history

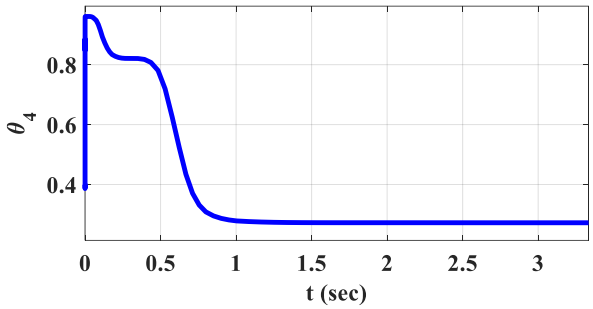

Figure 11. The θ_4 convergence time history

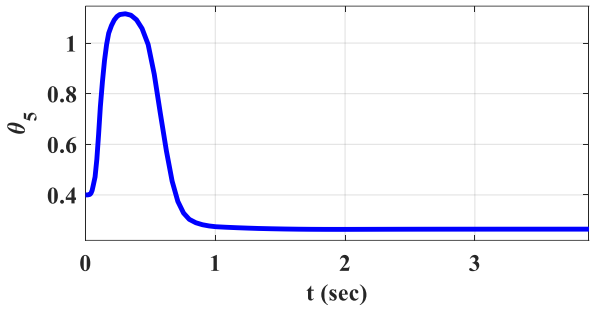

Figure 12. The θ_5 convergence time history

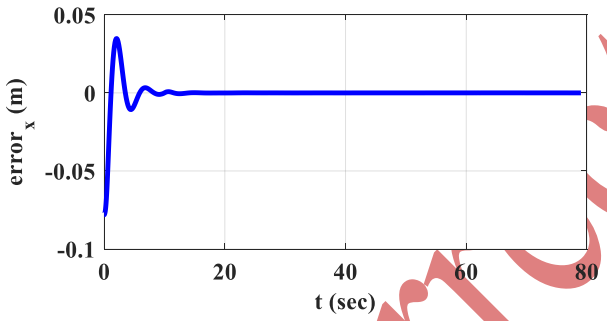

Figure 13. The x component of the reference trajectory tracking error considering disturbed input

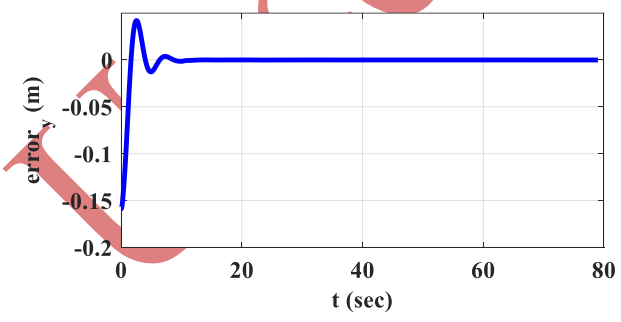

Figure 14. The y component of the reference trajectory tracking error considering disturbed input

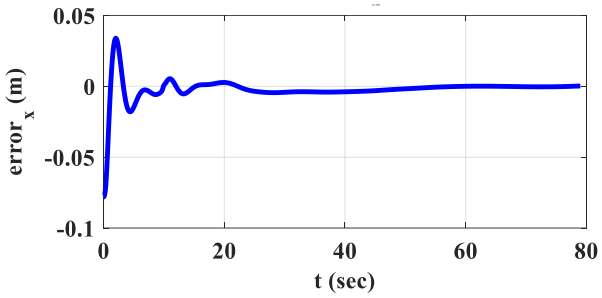

Figure 15. The x component of the reference trajectory tracking error considering step-shape disturbed input

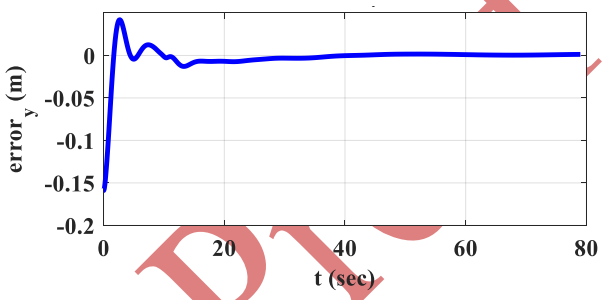

Figure 16. The x component of the reference trajectory tracking error considering step-shape disturbed input

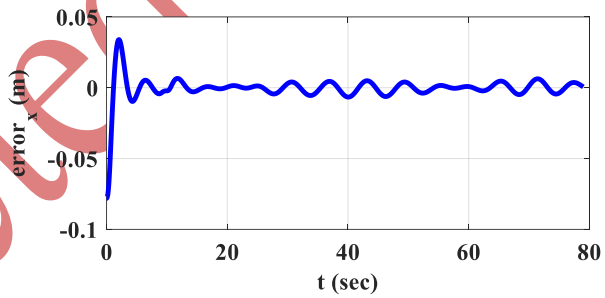

Figure 17. The x component of the reference trajectory tracking error considering sin-shape disturbed input

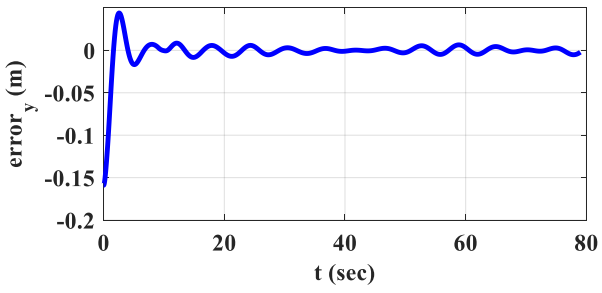

Figure 18. The y component of the reference trajectory tracking error considering sin-shape disturbed input

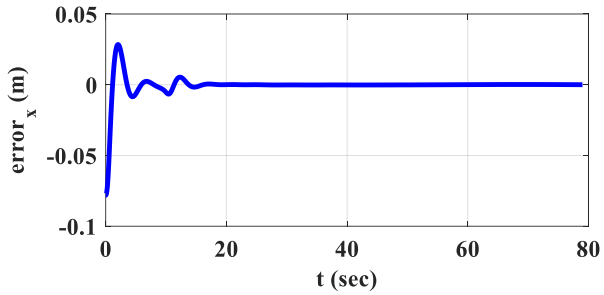

Figure 19. The x component of the reference trajectory tracking error considering uncertainy

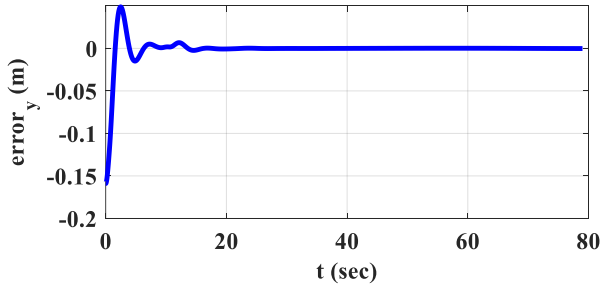

Figure 20. The y component of the reference trajectory tracking error considering uncertainy

5. Conclusions

In the present research, for the first time an adaptive partial feedback linearization approach was presented to trajectory tracking control of TTWRs. To this end, first an integrated model of the system kinematics, dynamics and actuator model was derived. Then, considering appropriate outputs using look-ahead method, the input-output feedback linearizing technique was employed. Since the exact value of some robot parameters may not be available in the controller, using RLS identification procedure, they were obtained. The obtained computer simulation results revealed the performance of the developed controller in terms of its accuracy and disturbance attenuation capability.

6. References

[1] K. Alipour and S. A. A. Moosavian, "Dynamically stable motion planning of wheeled robots for heavy object manipulation," *Advanced Robotics*, vol. 29, no. 8, pp. 545-560, 2015.

[2] K. Alipour, P. Daemi, A. Hassanpour, and B. Tarvirdizadeh, "On the capability of wheeled mobile robots for heavy object manipulation considering dynamic stability constraints," Multibody System Dynamics, vol. 41, no. 2, pp. 101-123, 2017.

[3] A. Mohamed, J. Ren, H. Lang, and M. El-Gindy, "Optimal path planning for an autonomous articulated vehicle with two trailers," International Journal of Automation and Control, vol. 12, no. 3, pp. 449-465, 2018.

[4] J. Yuan, S. Yang and J. Cai, " Consistent Path Planning for On-Axle-Hitching Multi-Steering Trailer Systems," IEEE Transactions on Industrial Electronics, 2018.

[5] K. Hou, Y. Zhang, J. Shi, and Y. Zheng, "Motion Planning Based on Artificial Potential Field for Unmanned Tractor in Farmland," International Conference on Applied Human Factors and Ergonomics, pp. 153-162, Springer, Cham, 2018.

[6] B. Siciliano and O. Khatib, (Eds.), Springer handbook of robotics, 2nd ed., Springer, 2016.

[7] A. B. Robat, K. Alipour, B. Tarvirdizadeh, and N. M. Aftah, "Trajectory tracking of a tractor-trailer robot using model predictive control," Modares Mechanical Engineering, vol. 17, no. 11, pp. 210-218, 2018.

[8] A. K. Khalaji, and S. A. A. Moosavian, "Robust adaptive controller for a tractor–trailer mobile robot," IEEE/ASME Transactions on Mechatronics, vol. 19, no. 3, pp. 943-953, 2014.

[9] A. K. Khalaji, and S. A. A. Moosavian, "Modified transpose Jacobian control of a tractor-trailer wheeled robot," Journal of Mechanical Science and Technology, vol. 29, no. 9, pp. 3961-3969, 2015.

[10] A. Khanpoor, A. K. Khalaji, and S. A. A. Moosavian, "Modeling and control of an underactuated tractor–trailer wheeled mobile robot," Robotica, vol. 35, no. 12, pp. 2297-2318, 2017.

[11] Y. Yu Lwin, and Y. Yamamoto. "Obstacle-responsive navigation scheme of a wheeled mobile robot based on look-ahead control." Industrial Robot: An International Journal, vol. 39, no. 3, pp. 282-293, 2012.

[12] B. Siciliano, L. Sciavicco, L. Villani, and G. Oriolo, "Robotics: modelling, planning and control," Springer Science & Business Media, 2010.

[13] J. J. Craig, "Introduction to robotics: mechanics and control," 3rd ed., Upper Saddle River, NJ, USA:: Pearson/Prentice Hall, 2005.

[14] S. Haykin "Adaptive Filtering Theory," Prentice Hall, 2013.